CERN-PH-TH/2014-037

Enhancing the $t\bar{t}H$ signal through top-quark spin polarization effects at the LHC

Sanjoy Biswas[a,b], **Rikkert Frederix**[c], **Emidio Gabrielli**[d,e,f], **and Barbara Mele**[b]

(a) Dipart. di Fisica, Università di Roma "La Sapienza", Piazzale Aldo Moro 2, I-00185 Rome, Italy

(b) INFN, Sezione di Roma, Piazzale Aldo Moro 2, I-00185 Rome, Italy

(c) PH Department, TH Unit, CERN, CH-1211 Geneva 23, Switzerland

(d) Department of Physics, University of Trieste, Strada Costiera 11, I-34151 Trieste, Italy

(e) NICPB, Ravala 10, Tallinn 10143, Estonia

(f) INFN, Sezione di Trieste, Via Valerio 2, I-34127 Trieste, Italy

arXiv:1403.1790v3 [hep-ph] 20 Oct 2014

ABSTRACT

We compare the impact of top-quark spin polarization effects in Higgs boson production in association with top-quark pairs and in corresponding backgrounds at the LHC. Because of the spin-zero nature of the Higgs boson, one expects, in the chiral limit for the top quarks, a substantial complementarity in $t\bar{t}$ spin correlations for a Higgs decaying into fermions/gauge-bosons and $t\bar{t}$ spin correlations for the corresponding irreducible $t\bar{t}f\bar{f}/VV$ backgrounds. Although top mass effects in $t\bar{t}H$ production are in general dominant, and seriously spoil the chiral-limit expectations, one can find observables that capture the $t\bar{t}$ angular spin correlations and can help in separating the signal from irreducible backgrounds. In particular, we show that, for both $H \to b\bar{b}$ and $H \to \gamma\gamma$, taking into account $t\bar{t}$ spin correlations in $t\bar{t}H$ production and irreducible backgrounds could appreciably improve the LHC sensitivity to the $t\bar{t}H$ channel.

1 Introduction

After the Higgs boson discovery in 2012 [1],[2], with m_H around 125 GeV, the LHC experiments are due to test the new particle properties at the highest possible accuracy in the forthcoming years. The direct verification of the Yukawa sector describing the Higgs couplings to fermions in the standard model (SM) plays a major role in establishing the actual nature of the observed new particle. The Higgs coupling Y_t to the top quark, the heaviest fermion, is of particular phenomenological and theoretical interest, since on the one hand it rules the dominant one-loop production mechanism $gg \to H$, and, on the other hand, it governs the leading Higgs-mass corrections dependence on the theory cut-off energy scale, connected to the scalar-field naturalness problem in the SM.

Potential contributions from new virtual states circulating in the $gg \to H$, possibly induced by some unknown new physics, make the Higgs-top coupling determination through $gg \to H$ production particularly model dependent. A model-independent test of the Y_t coupling relies instead on lower cross-section processes, notably the Higgs boson production in association with a top-quark pair $pp \to t\bar{t}H$ [3]-[13], where one can tag the actual presence of top quarks in the final state [14]-[15].

The $t\bar{t}H$ production is a very challenging channel, traditionally thought to require the highest LHC collision energies and integrated luminosities in order to be discriminated from background. The $t\bar{t}H$ cross section at 8-TeV pp collisions is quite depleted by the phase space of three heavy final particles, being just about 130 fb [16]. Nevertheless, both the ATLAS and CMS experiments have been performing better than expected, delivering a first set of quite constraining measurements of $t\bar{t}H$ signal strengths for different Higgs decay channels [17]-[22]. Dedicated analysis have been done even in the rarest channels, like $H \to \gamma\gamma$ and multileptons, where a more favorable signal-to-background ratio (S/B) compensates for the lack of statistics. The latter turn out to have a constraining power similar to the highest-statistics channels. For instance, with the present data set of about 5 fb^{-1} at 7 TeV plus about 20 fb^{-1} at 8 TeV, a 95% C.L. observed upper limit of 5.4 (5.3) times the SM cross section in the $H \to \gamma\gamma$ channel has been set by CMS [20] (ATLAS [18]), that is quite close to the corresponding upper bound for the $H \to bb$ channel based on the same data set by CMS [21].
By combining the $H \to bb, \gamma\gamma, \tau\tau$ and multileptons analyses [20]-[22], CMS already delivered a first measurement of the $t\bar{t}H$ signal strength, based on the total present data set, as $\sigma/\sigma_{SM} \simeq 2.5^{+1.1}_{-1.0}$, assuming SM Higgs branching ratios [23].

The channel with highest statistic, arising from $H \to b\bar{b}$, suffers from large QCD backgrounds, mainly corresponding to the $t\bar{t}b\bar{b}$ and $t\bar{t}jj$ final states. The reconstruction of the $H \to b\bar{b}$ resonance is also plagued by a combinatorial background arising from incorrect b-jet assignment (due either to extra b's from t and $\bar{t}$ decays or misidentified light jets). The $t\bar{t}jj$ reducible background component amounts to more than 95% of the total [24], and can be normalized through control regions not contaminated by the signal. Requiring multiple b-jet tagging is also very effective in reducing it. On the other hand, the irreducible $t\bar{t}b\bar{b}$ component is hard to separate or fit through data-driven methods, being much smaller than, and kinematically very similar to, the dominant $t\bar{t}jj$. As a consequence, in order to separate the irreducible

background, it is crucial to reach the highest possible control of theory predictions for the $t\bar{t}b\bar{b}$ production. To this end, in [24] an up-to-date discussion on the consistent interfacing next-to-leading-order (NLO) QCD perturbative predictions [25]-[29][1] with parton showers at 14 TeV is presented. After applying, a particular set of cuts optimizing the signal to background ratio, present analysis foresee $S/B \lesssim 1/20$. Developing strategies aimed to better discriminate the $t\bar{t}H$ signal distributions versus the irreducible $t\bar{t}b\bar{b}$ background is hence crucial, particularly in view of the much higher statistics that will be accumulated in forthcoming years at 14 TeV.

The scope of the present study is to explore the potential of the spin-correlation properties in the associated Higgs top-pair production at the LHC as a possible tool to improve the separation of the signal from the $t\bar{t}H$ irreducible backgrounds. The $t\bar{t}H$ spin properties have recently been considered in the literature as a mean to characterize a SM signal versus possible non-SM effects. In particular, spin correlations could help in disentangling the SM scalar component from a pseudoscalar contribution in the top-Higgs coupling [33]. In [34] it was emphasized that the relative impact of spin correlations on the leading-order (LO) $t\bar{t}H$ lepton kinematical distributions is much more dramatic than the one of the corresponding QCD NLO corrections [12].

The top quark is unique among all quarks, its life time being shorter than the characteristic hadronization time scale. Top quarks are then expected to decay before their original spin is affected by strong interactions, so ensuring that spin polarization at production level is fully transferred to the top decay products. Hence, by reconstructing the individual top systems (which can actually be done even in presence of two neutrinos in the final state [35]), the top-quark spin properties can be accessed by measuring angular distributions of the final decay products in $t \to W + b \to \ell\nu(du) + b$ [36]. Among the top decay products, the charged lepton (or d quark) has the maximal spacial correlation with the original top-quark spin axis [37]-[38].

Although in the SM top quark and antiquark pairs are mostly unpolarized in $\bar{t}t$ production at hadron colliders, their spins are strongly correlated [39]-[41], as confirmed by present experimental studies at the Tevatron [42],[43] and the LHC [35],[44].

In a naive picture, in the chiral limit of vanishing top-quark mass (or for very high invariant masses of the $t\bar{t}$ system, $m_{tt} \gg m_t$) the top quark and antiquark spins are highly correlated and parallel to each other along the $t\bar{t}$ production axis. Top pairs are hence produced in the LR + RL helicity configurations, where L(R) stands for the left(right)-handed helicity polarization. In the same kinematical limits, when the $t\bar{t}$ is produced in association with a Higgs boson, the top quark and antiquark helicities are also correlated, but in a complementary way with respect to the previous case. Indeed the Higgs-boson emission from the top-quark final states via Yukawa interactions induces a chirality flip in the top-quark polarization. Then, in contrast with $t\bar{t}$ production, for large m_{tt} invariant masses the dominant $t\bar{t}$ helicity configurations in the $t\bar{t}H$ final state will be LL+RR, while the LR+RL configuration is expected to be suppressed by terms of order $\mathcal{O}(m_t^2/m_{tt}^2)$.

We can now extend the same top-quark chiral limit to the irreducible backgrounds for

[1] See also [30]-[32] for NLO QCD corrections to $t\bar{t}jj$.

$t\bar{t}H$. For $H \to \gamma\gamma$, the irreducible background arises from direct $t\bar{t}\gamma\gamma$ production. In this case, the emission of photons from the quark lines in the $gg \to t\bar{t}$ and $q\bar{q} \to t\bar{t}$ amplitudes is not expected to affect the basic LR+RL helicity correlation of the plain top-quark pair production. One then should have some complementarity in the spin-correlation properties of the $t\bar{t}H(\to \gamma\gamma)$ signal and the ones of the $t\bar{t}\gamma\gamma$ irreducible background. As for the decay channel $H \to b\bar{b}$, the $t\bar{t}H(\to b\bar{b})$ signal presents of course the same spin correlations as the ones in the $t\bar{t}H(\to \gamma\gamma)$ channel. On the other hand, the analysis of the $t\bar{t}b\bar{b}$ irreducible background is less straightforward than in $t\bar{t}\gamma\gamma$ even in the top chiral limit, since many different topologies (presenting in general different $t\bar{t}$ spin correlations) contribute to the $t\bar{t}H(\to b\bar{b})$ amplitude. Nevertheless, one expects that the action of the Yukawa coupling in the signal channel should leave some imprint diversifying the signal polarization features of $t\bar{t}H(\to b\bar{b})$ with respect to the $t\bar{t}b\bar{b}$ irreducible background also in this case.

Just as it actually happens for the $t\bar{t}$ production [45], when dropping the unrealistic (for LHC energies) top chiral-limit assumption, predicting polarization properties of the $t\bar{t}H$ signal and corresponding backgrounds gets much harder. Top mass effects are indeed dominant in the bulk production of top pair systems. In $t\bar{t}$ production, the structure of spin correlations changes significantly over the top production phase space, with modulations (arising from the interference of different helicity states) that widely vary from threshold production to boosted-top regime [46]. As a consequence, the top-antitop spin-correlation properties in $t\bar{t}H$ and corresponding irreducible backgrounds are in general not simple to predict on the basis of the previous naive arguments.

In this paper, we study LO distributions of top decay products in $t\bar{t}H$ versus corresponding irreducible backgrounds, by keeping the correct correlation effects between top polarization in production and decay. We try to identify polarization observables that are particularly sensitive to separate the signal from irreducible backgrounds. The dependence on the reference-frame choice is also discussed.

We focus on the two channels corresponding to the $H \to \gamma\gamma$ and $H \to b\bar{b}$ decays

$$pp \to t\,\bar{t}\,H\,(\to \gamma\gamma) \tag{1}$$
$$pp \to t\,\bar{t}\,H\,(\to b\bar{b})\,, \tag{2}$$

where the corresponding irreducible backgrounds $t\bar{t}\gamma\gamma$ and $t\bar{t}b\bar{b}$ are expected to play a major role with respect to reducible ones.

Note that, regarding the $t\bar{t}\gamma\gamma$ background, there are extra contributions to the observed final state $\ell\nu b\ \ell\nu b\ \gamma\gamma$ due to photon brehmsstralung from charged top decay products [47]. The latter can fake the irreducible $t\bar{t}\gamma\gamma$ background, and affect the reconstruction of the spin properties of $t\bar{t}$ pairs. Proper kinematical cuts on the decay products of the top quarks can help to reduce these contributions, although eventual $t\bar{t}$ spin correlations are in general quite affected by kinematical cuts[2]. NLO QCD corrections to $t\bar{t}\gamma\gamma$ could be further incorporated through the MadGraph5_aMC@NLO framework [48].

[2]Similarly, b pairs generated via gluon radiation from b arising in top decays give extra contributions to the $\ell\nu b\ \ell\nu b\ b\bar{b}$ background from $t\bar{t}b\bar{b}$. The latter mildly contribute due to the corresponding low $b\bar{b}$ invariant mass.

In the Section 2, we start with a more quantitative analysis of the polarization effects in the $t\bar{t}H$ production. We then proceed to a detailed analysis of the signal and corresponding irreducible backgrounds for $H \to \gamma\gamma$ and $H \to b\bar{b}$, in Section 3 and 4, respectively. We then draw our conclusions in the Section 5.

2 Spin correlations in $t\bar{t}H$ production

Before entering the details of the signal and background analysis for the $t\bar{t}H$ production, we show in Fig. 1, the integrated top p_T distributions projected on the $t\,\bar{t}$ LL+RR and LR+RL helicity configurations (normalized to the total cross section), for the $t\bar{t}$ (left plot) and $t\bar{t}H$ (right plot) productions, in the Lab frame. Here, p_T^{top} is the minimum transverse momentum of the hardest top. We can see that helicity correlations as a function of p_T^{top} (which is directly

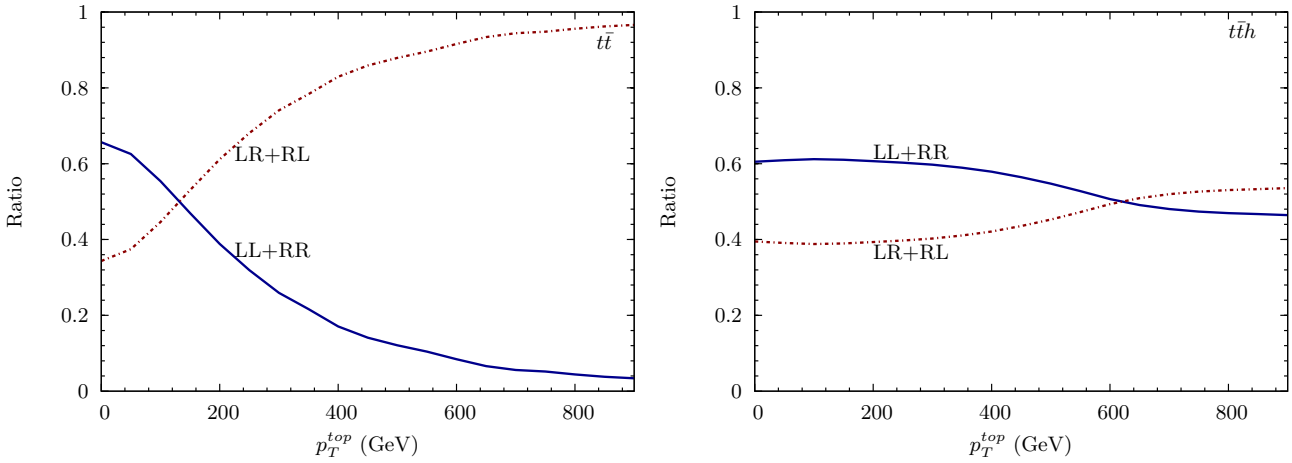

Figure 1: Integrated p_T distributions for the like-helicity top pairs ($t_L\bar{t}_L + t_R\bar{t}_R$) and unlike-helicity top pairs ($t_L\bar{t}_R + t_R\bar{t}_L$) in unpolarised $t\bar{t}$ (left plot) and $t\bar{t}h$ (right plot) samples, versus the hardest-top p_T cut at c.m. energy of 14 TeV, in the Lab frame.

connected to the invariant mass m_{tt} of the $t\bar{t}$ system adopted before) for $t\bar{t}$ and $t\bar{t}H$ productions are not complementary as in the top chiral limit, but present a quite different behavior. In $t\bar{t}$ production, one indeed observes the chiral limit emerging at large p_T^{top}, with the LR+RL component saturating the production rate. On the other hand, in the $t\bar{t}H$ production one does not have a complementary LL+RR dominance at high p_T^{top} as expected from the Higgs-sstralung chirality flip discussed in Section 1. Top mass effects and the presence in the final state of a further massive (Higgs) particle makes the LL+RR and LR+RL helicity components in $t\bar{t}H$ less unbalanced in all the statistically relevant top transverse-momentum range. One expects that the actual chiral limit is reached in $t\bar{t}H$ production for much higher p_T^{top} values than the ones that can be experimentally covered with the actual LHC energy and luminosity. While in $t\bar{t}$ production the fraction of the chiral-limit LR+RL configuration is above 80% for $p_T^{top} \gtrsim 400$

GeV, in $t\bar{t}H$ it moderately gets the upperhand for $p_T^{top} \gtrsim 600$ GeV, effectively dampened by Higgs radiation.

We then compare the fraction of LL+RR and LR+RL helicity configurations that contribute to the total $t\bar{t}H$ cross section, with the corresponding fractions in the irreducible backgrounds corresponding to the $H \to \gamma\gamma$ and $H \to bb$ channels. We find that about 61% of the total $t\bar{t}H$ cross section corresponds to the LL+RR combination, with a remaining 39% for LR+RL. Regarding the $t\bar{t}\gamma\gamma$ background (with basic cuts defined in the Fig. 2 caption later on), we have 28% of the total cross section with LL+RR combination, and a remaining 72% for LR+RL. As for the $t\bar{t}b\bar{b}$ background (with basic cuts defined in the Fig. 7 caption later on), we have an almost equal fraction of LL+RR and LR+RL configurations. One can see that in the $t\bar{t}\gamma\gamma$ background one indeed finds an opposite trend in the helicity configurations with respect to the $H \to \gamma\gamma$ signal. In the $t\bar{t}b\bar{b}$ background the effect is washed out in the integrated cross section.

We now proceed to scrutinize the effects of $t\bar{t}H$ top spin properties through the study of angular variables involving decay products of the top pair into two semileptonic final states $t \to b\ell\nu$, $\bar{t} \to \bar{b}\ell\nu$. We will focus in particular on charged-lepton pair and b-jet pair variables, where the b jets originate from top and antitop decays, applying strategies previously explored in $t\bar{t}$ production.
Spin correlations in hadronic $t\bar{t}$ production can be measured by studying angular distributions of top decay products in specific frames and coordinate basis [39]-[41]. The following observables and corresponding distributions have been extensively used[3]:

- Double polar decay distributions ($\frac{d^2\sigma}{d\cos\theta\, d\cos\bar{\theta}}$), where θ ($\bar{\theta}$) is the polar angle of any of the top (antitop) decay products.
- Distributions of three-dimensional opening angles (φ) between one top decay products and one anti-top decay products ($\frac{d\sigma}{d\cos\varphi}$).
- More compact one-dimensional observables given by combinations of azimuthal angles $\phi \pm \bar{\phi}$ of two top and antitop decay products ($\frac{d\sigma}{d(\phi\pm\bar{\phi})}$).

In this work we focus on the second kind of observables as they capture most of the $t\bar{t}$-system spin-correlation effects at moderate values of the top-quark p_T [46]. Apart from the laboratory frame, we will consider two further reference frames. The latter, although unusual, have been introduced in [40], being particularly sensitivite to the $t\bar{t}$ spin correlations compared to the lab frame.

We define the angle between the direction of flight of ℓ^+ (b) in the t rest system and ℓ^- ($\bar{b}$) in the $\bar{t}$ rest system [40]. Two different rest systems are involved in the above angular-variable definition, and to avoid ambiguities one has to specify the common initial frame where Lorentz boosts are applied to separately bring the t and $\bar{t}$ at rest.

The two aforementioned frames are defined as follows. The t and $\bar{t}$ rest systems are obtained by two corresponding rotation-free Lorentz boosts :

[3]For a recent discussion, see[46].

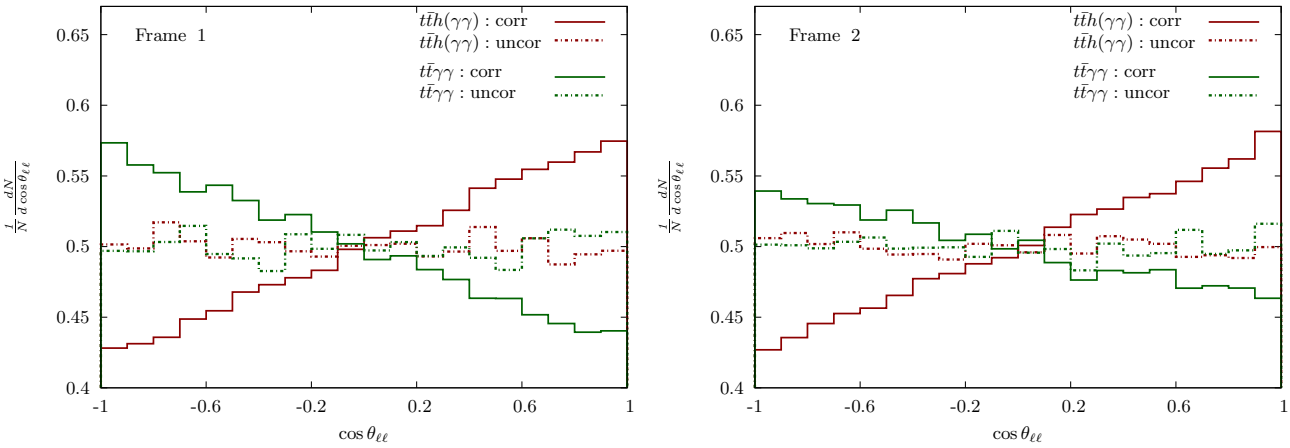

Figure 2: The $\cos\theta_{\ell\ell}$ distribution for the signal $t\bar{t}H(H \to \gamma\gamma)$ (red) and $t\bar{t}\gamma\gamma$ background (green), with (solid) and without (dashed) spin information, in Frame 1 (left) and Frame 2 (right). The cuts $p_T^{\gamma_{1,2}} > 20$ GeV, $|\eta_{\gamma_{1,2}}| < 2.5$ and $\Delta R_{\gamma_1\gamma_2} > 0.4$ have been imposed on photons, in addition to the invariant mass cut 123 GeV $< m_{\gamma\gamma} <$ 129 GeV.

- (Frame-1) with respect to the $t\bar{t}$-pair c.m. frame,
- (Frame-2) with respect to the laboratory frame.

In this paper we analyze the $t\bar{t}$ spin-correlations in both signal and background for two relevant Higgs decay channels $H \to \gamma\gamma$ and $H \to b\bar{b}$. For both signal and background the $t \to b\ell\nu$ decay has been performed in MadGraph5 [49] by retaining the full spin information, while in the uncorrelated case, the decay has been included by interfacing MadGraph5 with PYTHIA [50] at the $t\bar{t}H$ level, so neglecting the spin polarization effects. In our analysis, we do not include shower nor hadronization effects. In the following, we will show the results for angular and rapidity distributions for the decay products of the top and antitop, in both the signal $t\bar{t}H$, with $H \to \gamma\gamma$ and $H \to b\bar{b}$, and corresponding irreducible backgrounds $t\bar{t}\gamma\gamma$ and $t\bar{t}b\bar{b}$, respectively.

The variables that we found particularly sensitive to spin correlations are $\cos\theta_{\ell\ell}$ and $\Delta\eta_\ell$ (with $\Delta\eta_\ell \equiv |\eta_{\ell^+} - \eta_{\ell^-}|$), where $\theta_{\ell\ell}$ is the three-dimensional polar angle between the ℓ^+ and ℓ^- directions of flight, and η_ℓ is the pseudo rapidity of individual leptons in a specific frame. Analogously, we adopt the $\cos\theta_{b\bar{b}}$ and $\Delta\eta_b$ variables (with $\Delta\eta_b \equiv |\eta_b - \eta_{\bar{b}}|$) involving the two b quarks from t and $\bar{t}$ decays. This set of variables has been pinpointed after a careful scrutiny including different proposals adopted in $t\bar{t}$ production studies [45],[46].

In all the following plots, the signal (background) distributions will be shown via red (green) lines, while spin-correlated (-uncorrelated) cases will be reported through solid (dashed) lines. All distributions are normalized to 1. In the following, in each case we will show distributions that we found to be particularly sensitive to spin effects.

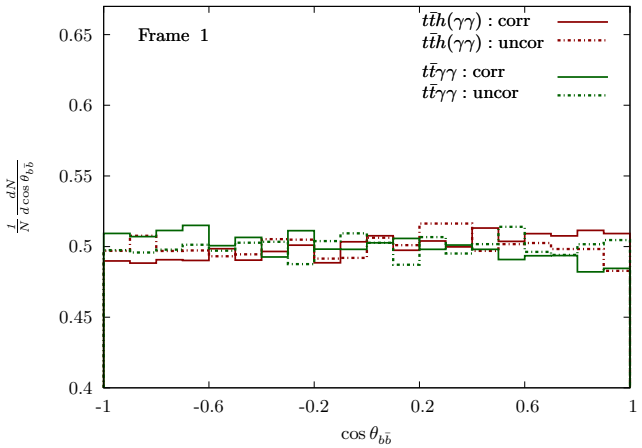

Figure 3: The $\cos\theta_{b\bar{b}}$ distribution for the signal $t\bar{t}H(H \to \gamma\gamma)$ (red) and $t\bar{t}\gamma\gamma$ background (green), with (solid) and without (dashed) spin information, in Frame 1. Same cuts as in Fig. 2 have been imposed.

3 The $t\bar{t}\gamma\gamma$ channel

Results for $t\bar{t}\gamma\gamma$ are shown in Figs. 2-6. Distributions in Figs. 2-4 include in the irreducible background only the photons emitted by initial and final charged states in the $gg, q\bar{q} \to t\bar{t}$ partonic precesses. In Figs. 5-6, the contributions from photons emitted by the t and $\bar{t}$ charged decay products are also included.

In Fig. 2, we show the $\cos\theta_{\ell\ell}$ distributions for $t\bar{t}\gamma\gamma$ signal and irreducible background with and without correlations in the $t, \bar{t}$ spin polarizations. In the left and right plots we report the results in the Frame-1 and Frame-2, respectively, as defined above. Here, we impose just the following kinematical cuts on the photons transverse momenta, $p_T^{\gamma_{1,2}} > 20$ GeV, pseudo-rapidities, $|\eta_{\gamma_{1,2}}| < 2.5$, and isolation, $\Delta R_{\gamma_1\gamma_2} > 0.4$, in addition to a diphoton invariant mass cut 123 GeV $< m_{\gamma\gamma} <$ 129 GeV, where ΔR_{ij} is as usual $\Delta R_{ij} = \sqrt{\eta_{ij}^2 + \phi_{ij}^2}$, with $\eta_{ij}(\phi_{ij})$ the rapidity (azimuthal) separation.

In the uncorrelated analysis, the angular distributions for the signal and background are both flat in $\cos\theta_{\ell\ell}$, in both reference frames. On the contrary, when the spin information is taken into account, the signal and background distributions are different and almost complementary. In particular, the signal (background) distributions is monotonically increasing (decreasing) as a function of $\cos\theta_{\ell\ell}$. This is a consequence of the aforementioned complementarity in the $t\bar{t}$ helicity correlations of the signal and irreducible background for the $H \to \gamma\gamma$ channel, that we have previously discussed. Although the correlation effect is remarkable both in Frame-1 and Frame-2, the separation between the correlated $\cos\theta_{\ell\ell}$ distributions for signal and background is more enhanced in Frame-1, where one gets an improvement in S/B (computed by integrating angular distributions over the range $0 < \cos\theta_{\ell\ell} < 1$) of about 17%, compared to the uncorrelated case.

In Fig. 3 , we show the corresponding distributions in the $\cos\theta_{b\bar{b}}$ variable in Frame-1 (analogous results hold in Frame-2). The distributions are all approximately flat, and no significant effect is found in this case.

In Fig. 4, for comparison, we consider various distributions in the laboratory frame, where the variables studied are more straightforward to reconstruct experimentally. We analyze the correlated and uncorrelated distributions in $\cos\theta_{\ell\ell}$ and $\Delta\eta_\ell$ (top), and $\cos\theta_{b\bar{b}}$ and $\Delta\eta_b$ (bottom) (with $\Delta\eta_\ell \equiv |\eta_{\ell^+} - \eta_{\ell^-}|$), $\Delta\eta_b \equiv |\eta_b - \eta_{\bar{b}}|$). In all plots in the Lab Frame the inclusion of spin correlations increases the difference in distribution shapes between signal and background, although the relative effect is quite smaller than in Frame 1 and Frame 2 for leptonic distributions. The $\cos\theta_{b\bar{b}}$ distribution in the Lab Frame is instead much more effective in separating signal and background with respect to Frame 1 (where it is almost flat in all cases cf. Fig. 3). Distributions in rapidity separations turns out to be more selective in the $\Delta\eta_\ell < 1.5$ range.

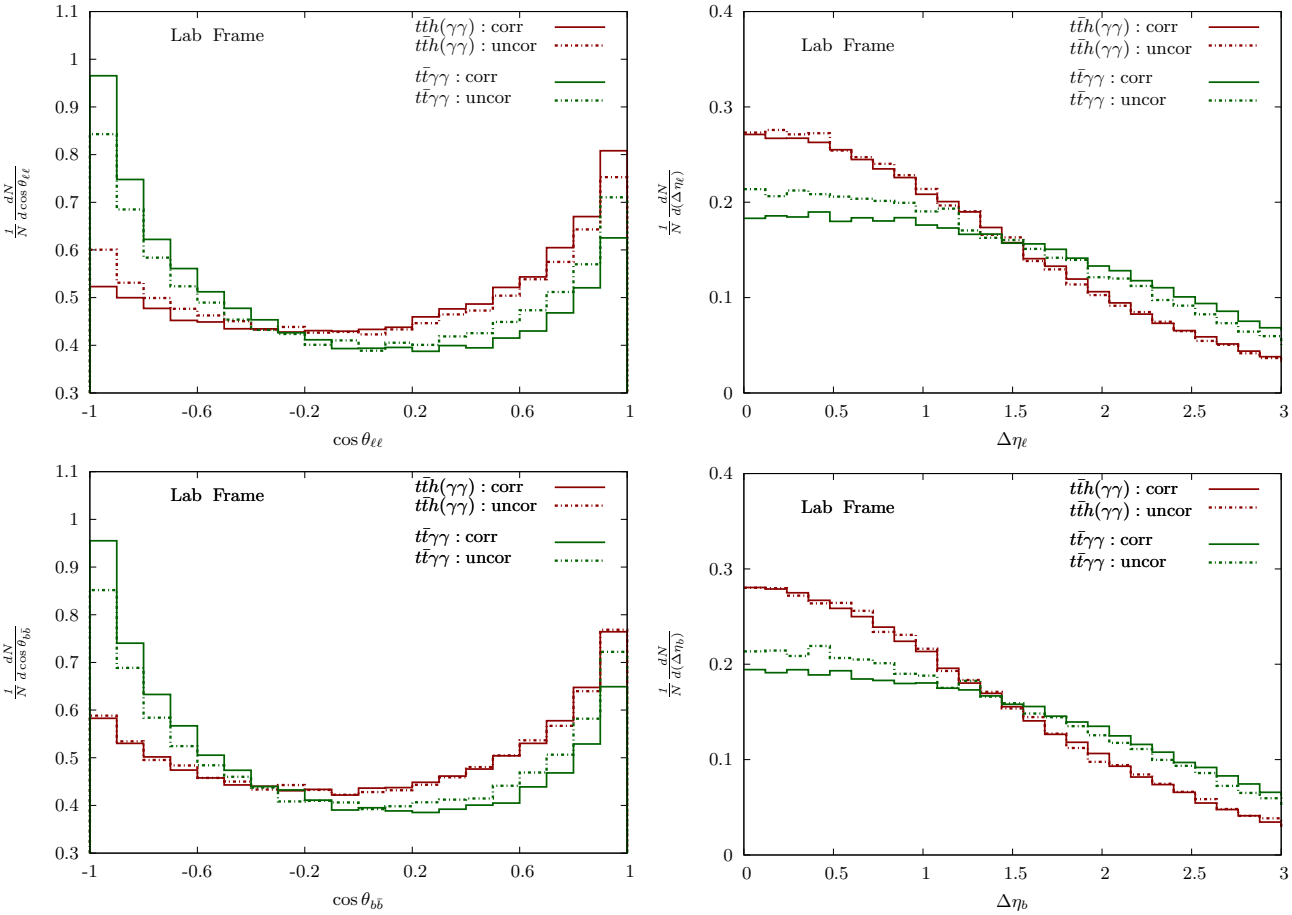

Figure 4: The $\cos\theta_{\ell\ell}$ (top left), $\Delta\eta_\ell$ (top right), $\cos\theta_{b\bar{b}}$ (bottom left), and $\Delta\eta_b$ (bottom right) distributions for the signal $t\bar{t}H(H \to \gamma\gamma)$ (red) and $t\bar{t}\gamma\gamma$ background (green), with (solid) and without (dashed) spin information, in the Lab frame. Same cuts as in Fig. 2 have been imposed.

Now, we consider the effects induced including the contributions of photon emissions from the t and $\bar{t}$ charged decay products in the irreducible $\gamma\gamma$ continuum. In order to do so, additional

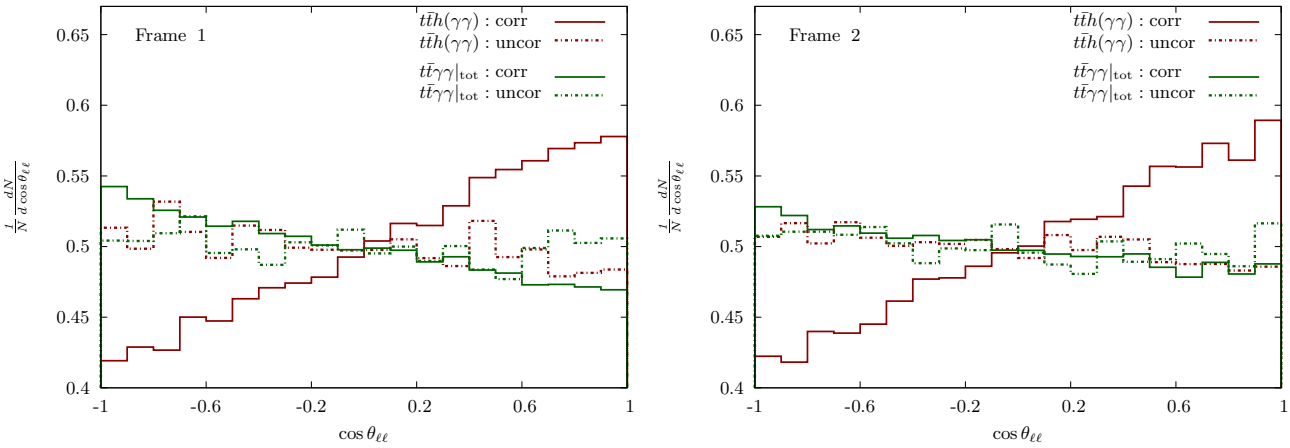

Figure 5: The $\cos\theta_{\ell\ell}$ distribution for the signal $t\bar{t}H(H\to\gamma\gamma)$ (red) and full $\gamma\gamma$ background (including radiation from t,$\bar{t}$ decay products, as defined in the text) (green), with (solid) and without (dashed) spin information, in Frame 1 (left) and Frame 2 (right). The set of cuts listed in Eq.(3-6) have been applied to both signal and background.

kinematic cuts are required for photon and b-jet isolation

$$p_T^{b,\gamma_{1,2}} > 20 \text{ GeV and } p_T^{\ell} > 10 \text{ GeV} \tag{3}$$

$$|\eta^b| < 4.7, |\eta^\ell| < 2.7 \text{ and } |\eta^\gamma| < 2.5 \tag{4}$$

$$\Delta R(bb, \ell\ell, \gamma\gamma, b\,\ell, b\gamma, \ell\gamma) > 0.4 \tag{5}$$

$$123 \text{ GeV} < m_{\gamma\gamma} < 129 \text{ GeV}\,. \tag{6}$$

In Fig. 5 we show the effects of including both photon radiation from t,$\bar{t}$ decay products and the new set of kinematical cuts defined in Eq.(3-6) on signal and background. We show the $\cos\theta_{\ell\ell}$ distributions in Frame-1 (left) and Frame-2 (right), to be compared to the ones not including extra background radiation in Fig. 2. One can see that the $\cos\theta_{\ell\ell}$ distributions for signal are basically unaffected by the new selection cuts, while in the background the extra photon radiation tends to reduce the gap between the correlated and uncorrelated $\cos\theta_{\ell\ell}$ distributions. In Frame-1 one gets an improvement by 14% in S/B.

In the Lab frame, Fig. 6 shows the $\cos\theta_{\ell\ell}$ (top left), $\Delta\eta_\ell$ (top right), $\cos\theta_{b\bar{b}}$ (bottom left) and $\Delta\eta_b$ (bottom right) distributions including extra photon radiation and new selection cuts. One can see that the effects of photon emission from the top decay products do not dramatically affect the previous results where these contributions where ignored (cf. Fig. 4). Differences are found mainly for low separations of lepton and b pairs (that is for $\cos\theta_{\ell\ell}, \cos\theta_{b\bar{b}} \sim 1$ and $\Delta\eta_\ell, \Delta\eta_b < 1$), where the new set of cuts is more effective. In conclusion, we find that the analysis of the $\cos\theta_{\ell\ell}$ distributions for the channel $t\bar{t}H(H\to\gamma\gamma)$ and its irreducible background in a study that correctly takes into account spin-correlation effects could significantly help in

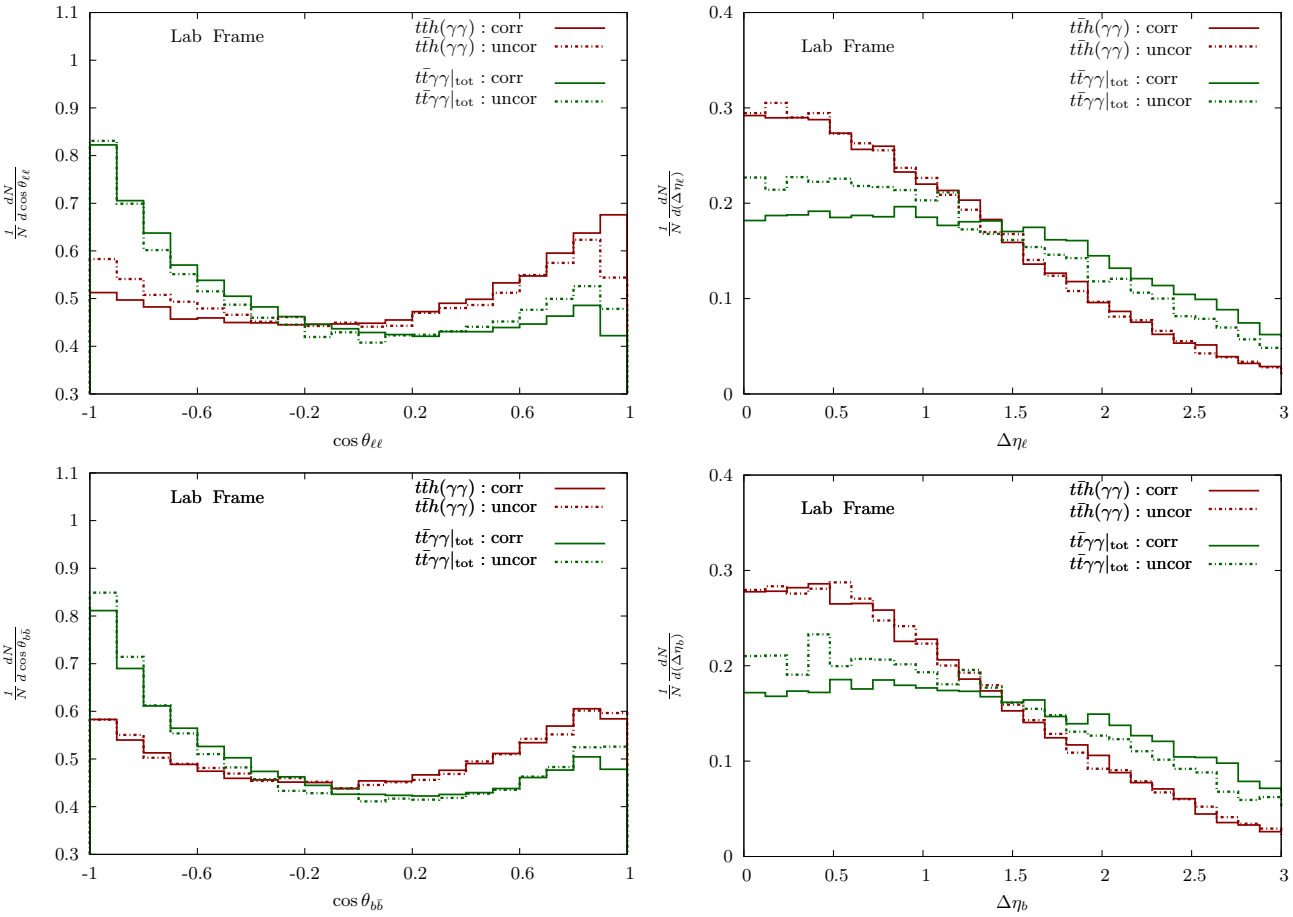

Figure 6: The $\cos\theta_{\ell\ell}$ (top left), $\Delta\eta_\ell$ (top right), $\cos\theta_{b\bar{b}}$ (bottom left), and $\Delta\eta_b$ (bottom right) distributions for the signal $t\bar{t}H(H \to \gamma\gamma)$ (red) and full $\gamma\gamma$ background (including radiation from $t\bar{t}$ decay products, as defined in the text) (green), with (solid) and without (dashed) spin information, in the Lab frame. Same cuts as in Fig. 5 have been imposed.

enhancing the signal-to-background ratio with respect to the uncorrelated analysis. The use of dedicated reference frames for reconstruction, like Frame-1 and Frame-2, can improve S/B by about 15%. More modest improvements can be obtained in the laboratory frame.

4 The $t\bar{t}b\bar{b}$ channel

We now turn to the spin-correlated analysis for $t\bar{t}H(H \to b\bar{b})$. With respect to the $H \to \gamma\gamma$ channel, here the $(t\bar{t}b\bar{b})$ irreducible background receives contributions from many components that have different top spin correlations. This makes even more difficult to guess by general arguments how the correlated/uncorrelated background distributions may behave, especially when kinematical cuts can affect predictions. We stress that the following analysis is an idealized one where we assume to be able to distinguish the b quarks coming from top (anti top) decays.

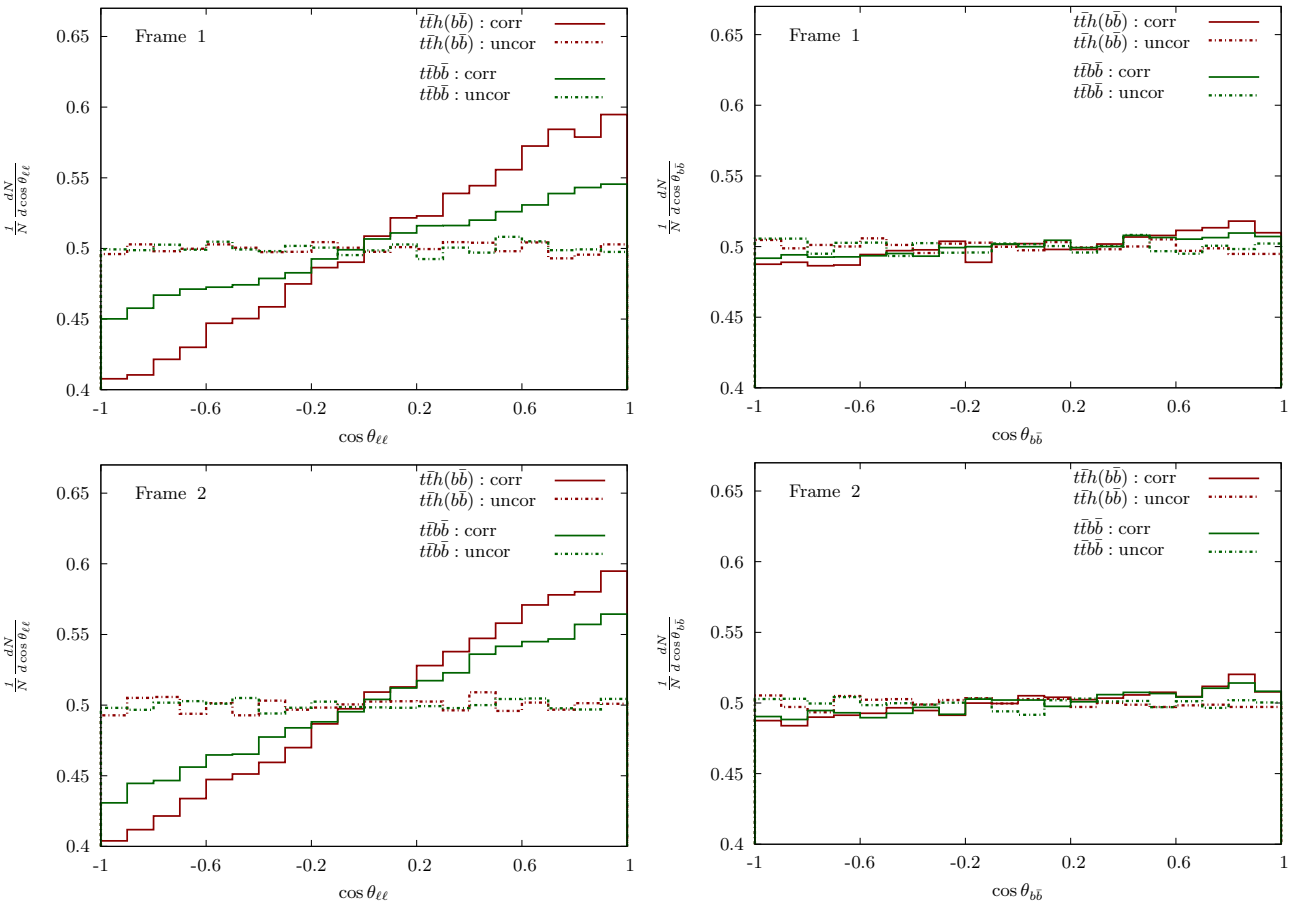

Figure 7: The $\cos\theta_{\ell\ell}$ (left) and $\cos\theta_{b\bar{b}}$ (right) distributions for the signal $t\bar{t}H(H \to b\bar{b})$ (red) and $t\bar{t}b\bar{b}$ background (green), with (solid) and without (dashed) spin information, in Frame 1 (top) and Frame 2 (bottom). The selection $p_T^{b,\bar{b}} > 20$ GeV, $|\eta_{b,\bar{b}}| < 2.5$ and $\Delta R_{b\bar{b}} > 0.4$ has been imposed on the two b-quarks not coming from t decays, in addition to the invariant mass cut $m_{b\bar{b}} > 100$ GeV.

In Fig. 7 we show the results for the $\cos\theta_{\ell\ell}$ (left) and $\cos\theta_{b\bar{b}}$ (right) distributions for signal and irreducible background, in Frame-1 (top) and Frame-2 (bottom). In both frames spin effects are quite relevant in the $\cos\theta_{\ell\ell}$ distributions. In particular, while the uncorrelated distributions are in general flat, both the correlated signal and background behaviors are monotonically increasing as a function of $\cos\theta_{\ell\ell}$, with a stronger slope in the signal case. On the other hand, the effect of spin correlations is extremely mild for $\cos\theta_{b\bar{b}}$ distributions in both Frame-1 and Frame-2.
Then, in the $t\bar{t}H(H \to b\bar{b})$ case, retaining the full spin information can still help in enhancing S/B, although not as much as in the case of the $H \to \gamma\gamma$ channel. In particular, in Frame-1, including spin correlations improves S/B by 4% using the $\cos\theta_{\ell\ell}$ variable, while a very small gain is obtained by using $\cos\theta_{b\bar{b}}$.

For comparison we present in Fig. 8 the corresponding results for the $\cos\theta_{\ell\ell}$ (top left), $\Delta\eta_\ell$ (top right), $\cos\theta_{b\bar{b}}$ (bottom left) and $\Delta\eta_b$ (bottom right) distributions in the laboratory frame.

Spin effects are quite milder in this case, too, and in general do not improve much the signal-background separation. Signal and background have similar distributions, in both correlated

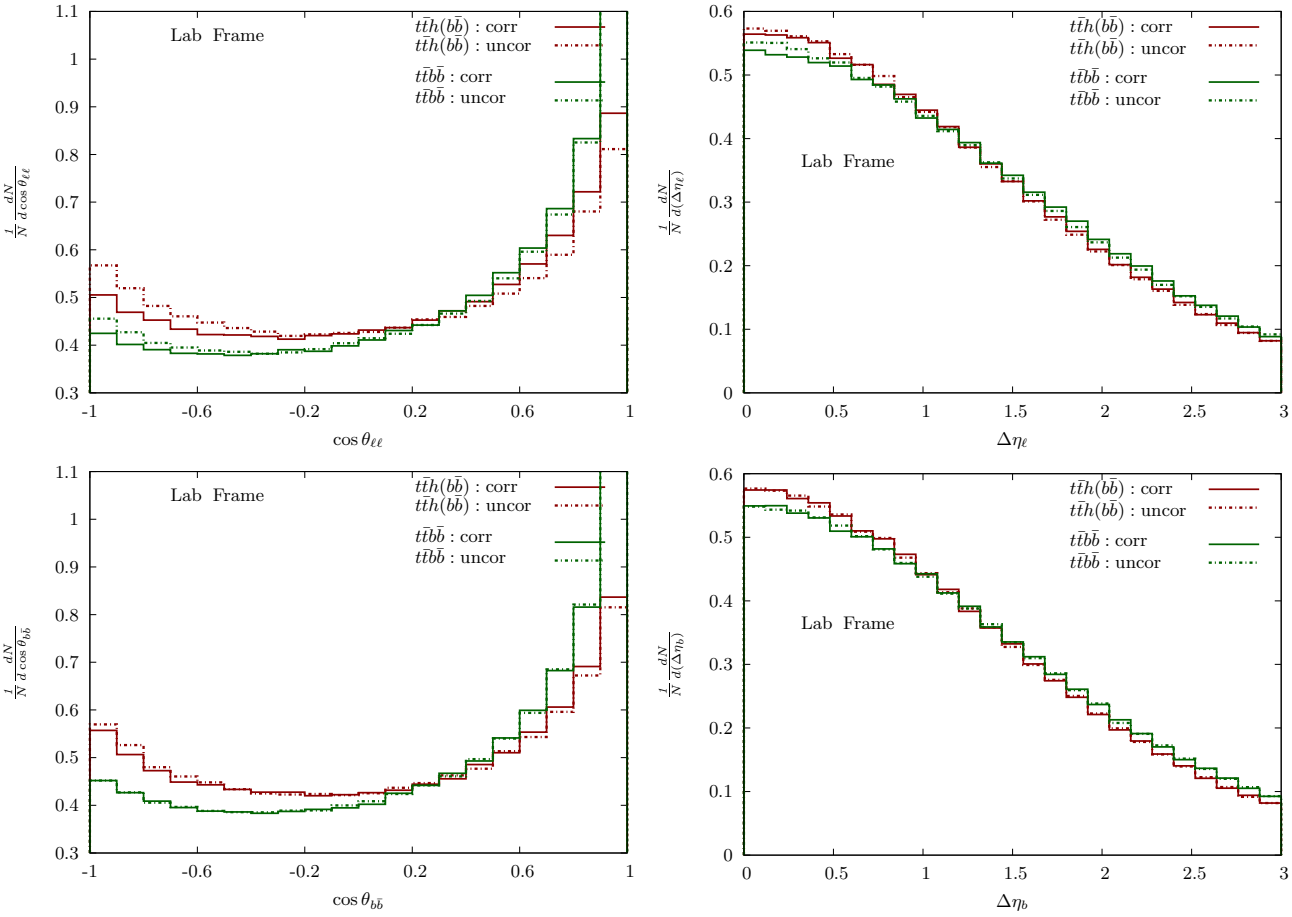

Figure 8: The $\cos\theta_{\ell\ell}$ (top left), $\Delta\eta_\ell$ (top right), $\cos\theta_{b\bar{b}}$ (bottom left), and $\Delta\eta_b$ (bottom right) distributions for the signal $t\bar{t}H(H \to b\bar{b})$ (red) and $t\bar{t}b\bar{b}$ background (green), with (solid) and without (dashed) spin information, in the Lab frame. Same cuts as in Fig. 7 have been imposed.

and uncorrelated cases. The advantage of employing a full spin-correlated analysis in the Lab frame looks quite modest.

Finally, in Fig. 9 we explore the boosted top regime, by imposing that the highest top p_T satisfies the cut $p_T > 250$ GeV in the laboratory frame. In particular, we plot the $\cos\theta_{\ell\ell}$ distributions for the signals $t\bar{t}H$ $(H \to \gamma\gamma)$ (left) and $t\bar{t}H$ $(H \to b\bar{b})$ (right) with their corresponding backgrounds $t\bar{t}\gamma\gamma$ and $t\bar{t}b\bar{b}$, imposing the cuts $p_T > 20$ GeV, $|\eta| < 2.5$ and $\Delta R > 0.4$ on the final state photons or b quarks (where b's are not from top decays) in addition to the invariant mass cut 123 GeV$< m_{\gamma\gamma} <$ 129 GeV, and $m_{b\bar{b}} > 100$ GeV, respectively. The left and right plots in Fig. 9 should be compared with the top-left plots of Fig. 4 and Fig. 8, respectively. Requiring a boosted top increases the lepton-pair angular separation in general. Then, in the $H \to \gamma\gamma$, one obtains practically identical uncorrelated curves, especially in the correlated case. There is instead some advantage for the $H \to b\bar{b}$ signal, where the separation of the $\cos\theta_{\ell\ell}$ distribu-

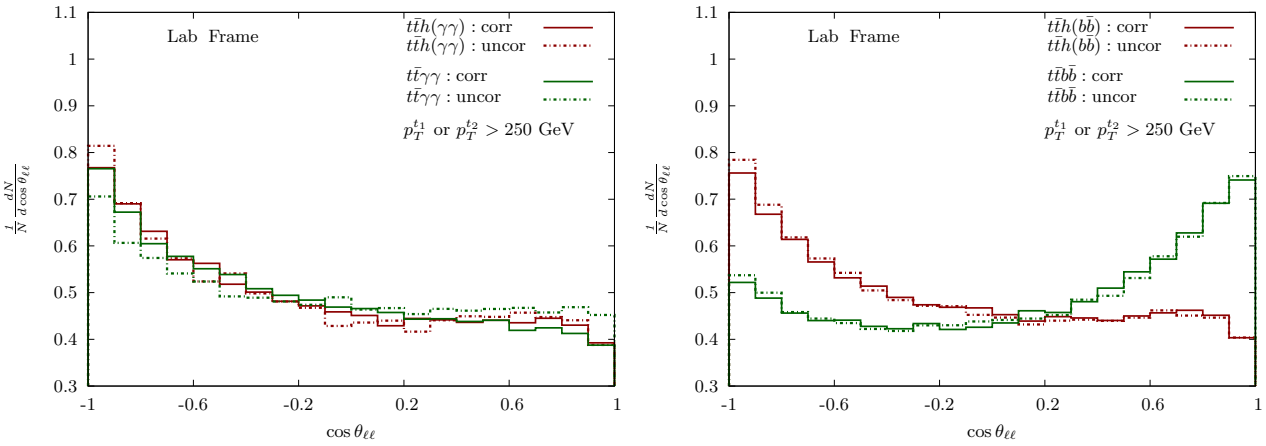

Figure 9: The $\cos\theta_{\ell\ell}$ distributions for the signals (red) $t\bar{t}H$ $(H \to \gamma\gamma)$ (left) and $t\bar{t}H$ $(H \to b\bar{b})$ (right) with their corresponding backgrounds (green) $t\bar{t}\gamma\gamma$ and $t\bar{t}b\bar{b}$ in the Lab frame, after demanding one highly-boosted top by imposing that the highest top p_T satisfies the cut $p_T > 250$ GeV. Same cuts as in Fig. 2 and 7 have been applied, respectively.

tions for signal and background increases both in the correlated and uncorrelated case. The spin-correlation effects are anyhow modest even in this case

Summing up, as for the $H \to \gamma\gamma$ signal, we can see that the most significant deviations between the correlated and uncorrelated analysis is observed in the $\cos\theta_{\ell\ell}$ distributions, evaluated in Frame-1 and Frame-2. On the other hand, for the $H \to b\bar{b}$ signal, the signal and background including spin correlations have similar (less distinctive) behaviors with respect to the $H \to \gamma\gamma$ case. Anyhow, also for the $H \to b\bar{b}$ signal, an analysis taking into account spin correlations in a suitable frame could significantly help in enhancing the S/B ratio with respect to the uncorrelated analysis.

5 Summary and Outlook

The top-quark polarization observables are quite powerful tools that can be used to enhance the sensitivity to the dynamics involved in the top-production processes. The main purpose of the present study was to investigate the advantages of taking into account the full $t\bar{t}$ spin-correlation effects in the measurement of the $t\bar{t}H$ process versus its irreducible backgrounds.

We found that, for the two processes $t\bar{t}H(H \to \gamma\gamma)$ and $t\bar{t}H(H \to b\bar{b})$, where irreducible backgrounds are bound to have a dominant role when increasing the LHC data set at 14 TeV, there are indeed angular variables defined in dedicated reference frames that could sizably increase the separation of signal and background, with a gain of up to 30% in S/B for $t\bar{t}H(H \to \gamma\gamma)$ in particular phase-space regions.

Of course, our study suffers from a series of limitations that one will have to address in order to assess the actual potential of the suggested optimization strategy:

– First, we just assumed a simplified framework not including NLO QCD corrections and parton-shower effects. In [34], one can see that NLO corrections tend to modify the (uncorrelated) signal in the same direction as the LO spin correlation effects. One should then also estimate the NLO corrections for the corresponding backgrounds, and confront them with spin effects.

– In the present study, we started to examine the effects of additional experimental kinematic selection cuts on spin correlations. We found that, in the $t\bar{t}H(H \to \gamma\gamma)$ channel, realistic cuts do not upset the correlation behavior. On the other hand, a general depletion of the spin effects is observed in the background case. We expect a similar sensitivity to further cuts in the $t\bar{t}H(H \to b\bar{b})$ case.

– We have assumed a 100% top-system reconstruction efficiency, although we are considering the challenging dilepton final state containing two neutrinos. Our results could then be quite optimistic. In a more realistic experimental set-up, the effects we found could be partly washed out by detection and resolution experimental effects, affecting the reconstruction of the two t and $\bar{t}$ rest frames. In [46], these issues were discussed for the $t\bar{t}$ production. In the $t\bar{t}h$ case, the lower production statistics will make the top reconstruction even harder. On the other hand, whenever one consider spin-correlation distributions in the Lab frame (cf. Fig. 4 and Fig. 8), the t and $\bar{t}$ rest frame reconstruction is not needed, and the spin-correlation results will not be deteriorated.

– In the $t\bar{t}H(H \to b\bar{b})$ case, we included only the irreducible $t\bar{t}b\bar{b}$ background, while by relaxing the b-tagging multiplicity the reducible light-jet $t\bar{t}jj$ channel becomes overwhelming. We checked how the latter background reacts to the inclusion of $t\bar{t}$ spin correlations by using similar selection criteria than the ones in the $t\bar{t}b\bar{b}$ analysis. We found that, in Frame 1, the $\cos\theta_{\ell\ell}$ distribution for $t\bar{t}jj$ is similar to the $t\bar{t}b\bar{b}$ distribution, and approaches the signal one. Spin correlations might then be as much effective as in the irreducible $t\bar{t}b\bar{b}$ channel for separating signal from background.

– In this study, we explored the spin correlations in the dilepton $t\bar{t}$ channel, which is only a subdominant component of the $t\bar{t}H$ sample. The possibility to include in spin-correlation studies the higher-rate lepton+jets channel was studied for $t\bar{t}$ production in [45, 46]. Although the $W \to jj$ light-jet analyzing power is on average smaller, and the light-jet identification can be nontrivial (implying shower and hadronization distortions), for the semi-leptonic $t\bar{t}$ system the top reconstruction turns out to be in general quite efficient. Similar techniques could be extended to the $t\bar{t}H$ production.

– The actual spin-correlation distributions of the $t\bar{t}H(H \to b\bar{b})$ signal will also be affected by the b-jet combinatorial background. A preliminary simulation that uses simplified assumption on top reconstruction effects (in particular a 10 GeV mass resolution on the two top ($\ell\nu b$) systems, and a 15 GeV resolution on the Higgs ($b\bar{b}$) system) results in : a) an extra 10% for the total event rates, and b) a few percents distortion effect on the signal $\cos\theta_{\ell\ell}$ distributions in Fig. 7, that tends to make the distribution slope flatter.

We conclude that spin-correlation features in the $t\bar{t}H$ production are quite promising for enhancing the signal sensitivity over the irreducible background. Hence, they should definitely

be studied in a more systematic way, and eventually be included in future analysis of the process at higher integrated luminosities.

Aknowledgments: S.B. would like to thank Satya Mukhopadhay for helpful discussions. E.G. would like to thank the CERN PH-TH division for its kind hospitality during the preparation of this work. This work was supported by the ESF grant MTT60, by the recurrent financing SF0690030s09 project and by the European Union through the European Regional Development Fund.

References

[1] G. Aad *et al.* [ATLAS Collaboration], "Observation of a new particle in the search for the Standard Model Higgs boson with the ATLAS detector at the LHC," Phys. Lett. B **716** (2012) 1 [arXiv:1207.7214 [hep-ex]].

[2] S. Chatrchyan *et al.* [CMS Collaboration], "Observation of a new boson at a mass of 125 GeV with the CMS experiment at the LHC," Phys. Lett. B **716** (2012) 30 [arXiv:1207.7235 [hep-ex]].

[3] Z. Kunszt, "Associated Production of Heavy Higgs Boson with Top Quarks," Nucl. Phys. B **247** (1984) 339.

[4] W. J. Marciano and F. E. Paige, "Associated production of Higgs bosons with $t\bar{t}$ pairs," Phys. Rev. Lett. **66** (1991) 2433.

[5] J. F. Gunion, "Associated top anti-top Higgs production as a large source of WH events: Implications for Higgs detection in the lepton neutrino gamma gamma final state," Phys. Lett. B **261** (1991) 510.

[6] W. Beenakker, S. Dittmaier, M. Kramer, B. Plumper, M. Spira and P. M. Zerwas, "Higgs radiation off top quarks at the Tevatron and the LHC," Phys. Rev. Lett. **87** (2001) 201805 [hep-ph/0107081].

[7] W. Beenakker, S. Dittmaier, M. Kramer, B. Plumper, M. Spira and P. M. Zerwas, "NLO QCD corrections to $t\bar{t}H$ production in hadron collisions," Nucl. Phys. B **653** (2003) 151 [hep-ph/0211352].

[8] L. Reina and S. Dawson, "Next-to-leading order results for $t\bar{t}H$ production at the Tevatron," Phys. Rev. Lett. **87** (2001) 201804 [hep-ph/0107101].

[9] S. Dawson, L. H. Orr, L. Reina and D. Wackeroth, "Associated top quark Higgs boson production at the LHC," Phys. Rev. D **67** (2003) 071503 [hep-ph/0211438].

[10] S. Dawson, C. Jackson, L. H. Orr, L. Reina and D. Wackeroth, "Associated Higgs production with top quarks at the large hadron collider: NLO QCD corrections," Phys. Rev. D **68** (2003) 034022 [hep-ph/0305087].

[11] S. Dittmaier, M. Kramer, 1 and M. Spira, "Higgs radiation off bottom quarks at the Tevatron and the CERN LHC," Phys. Rev. D **70** (2004) 074010 [hep-ph/0309204].

[12] R. Frederix, S. Frixione, V. Hirschi, F. Maltoni, R. Pittau and P. Torrielli, "Scalar and pseudoscalar Higgs production in association with a top-antitop pair," Phys. Lett. B **701** (2011) 427 [arXiv:1104.5613 [hep-ph]].

[13] M. V. Garzelli, A. Kardos, C. G. Papadopoulos and Z. Trócsányi, "Standard Model Higgs boson production in association with a top anti-top pair at NLO with parton showering," Europhys. Lett. **96** (2011) 11001 [arXiv:1108.0387 [hep-ph]].

[14] F. Maltoni, D. L. Rainwater and S. Willenbrock, "Measuring the top quark Yukawa coupling at hadron colliders via $t\bar{t}H, H \to W^+W^-$," Phys. Rev. D **66** (2002) 034022 [hep-ph/0202205].

[15] A. Belyaev and L. Reina, "$pp \to t\bar{t}H, H \to \tau\tau$: Toward a model independent determination of the Higgs boson couplings at the LHC," JHEP **0208** (2002) 041 [hep-ph/0205270].

[16] S. Dittmaier *et al.* [LHC Higgs Cross Section Working Group Collaboration], "Handbook of LHC Higgs Cross Sections: 1. Inclusive Observables," arXiv:1101.0593 [hep-ph].

[17] ATLAS Collaboration, "Search for the Standard Model Higgs boson produced in association with top quarks in proton-proton collisions at s = 7 TeV using the ATLAS detector," ATLAS-CONF-2012-135.

[18] The ATLAS collaboration, "Search for ttH production in the $H \to \gamma\gamma$ channel at $\sqrt{s} = 8$ TeV with the ATLAS detector," ATLAS-CONF-2013-080.

[19] S. Chatrchyan *et al.* [CMS Collaboration], "Search for the standard model Higgs boson produced in association with a top-quark pair in pp collisions at the LHC," JHEP **1305** (2013) 145 [arXiv:1303.0763 [hep-ex]].

[20] CMS Collaboration, "Search for ttH production in events where H decays to photons at 8 TeV collisions," CMS-PAS-HIG-13-015.

[21] CMS Collaboration, "Search for Higgs Boson Production in Association with a Top-Quark Pair and Decaying to Bottom Quarks or Tau Leptons," CMS-PAS-HIG-13-019.

[22] CMS Collaboration, "Search for the standard model Higgs boson produced in association with top quarks in multilepton final states," CMS-PAS-HIG-13-020.

[23] CMS Collaboration,
https://twiki.cern.ch/twiki/bin/view/CMSPublic/ttHCombinationTWiki

[24] S. Heinemeyer *et al.* [LHC Higgs Cross Section Working Group Collaboration], "Handbook of LHC Higgs Cross Sections: 3. Higgs Properties," arXiv:1307.1347 [hep-ph].

[25] A. Bredenstein, A. Denner, S. Dittmaier and S. Pozzorini, "NLO QCD corrections to $pp \to t\bar{t}b\bar{b} + X$ at the LHC," Phys. Rev. Lett. **103** (2009) 012002 [arXiv:0905.0110 [hep-ph]].

[26] A. Bredenstein, A. Denner, S. Dittmaier and S. Pozzorini, "NLO QCD Corrections to Top Anti-Top Bottom Anti-Bottom Production at the LHC: 2. full hadronic results," JHEP **1003** (2010) 021 [arXiv:1001.4006 [hep-ph]].

[27] G. Bevilacqua, M. Czakon, C. G. Papadopoulos, R. Pittau and M. Worek, "Assault on the NLO Wishlist: $pp \to t\bar{t}b\bar{b}$," JHEP **0909** (2009) 109 [arXiv:0907.4723 [hep-ph]].

[28] A. Kardos and Z. Trócsányi, "Hadroproduction of $t\bar{t}$ pair with a $b\bar{b}$ pair with PowHel," arXiv:1303.6291 [hep-ph].

[29] F. Cascioli, P. Maierhoefer, N. Moretti, S. Pozzorini and F. Siegert, "NLO matching for *ttbb* production with massive b-quarks," arXiv:1309.5912 [hep-ph].

[30] G. Bevilacqua, M. Czakon, C. G. Papadopoulos and M. Worek, "Dominant QCD Backgrounds in Higgs Boson Analyses at the LHC: A Study of $pp \to t\bar{t}+$ 2 jets at Next-To-Leading Order," Phys. Rev. Lett. **104** (2010) 162002 [arXiv:1002.4009 [hep-ph]].

[31] G. Bevilacqua, M. Czakon, C. G. Papadopoulos and M. Worek, "Hadronic top-quark pair production in association with two jets at Next-to-Leading Order QCD," Phys. Rev. D **84** (2011) 114017 [arXiv:1108.2851 [hep-ph]].

[32] S. Hoeche, F. Krauss, P. Maierhoefer, S. Pozzorini, M. Schonherr and F. Siegert, "Next-to-leading order QCD predictions for top-quark pair production with up to two jets merged with a parton shower," arXiv:1402.6293 [hep-ph].

[33] J. Ellis, D. S. Hwang, K. Sakurai and M. Takeuchi, "Disentangling Higgs-Top Couplings in Associated Production," arXiv:1312.5736 [hep-ph].

[34] P. Artoisenet, R. Frederix, O. Mattelaer and R. Rietkerk, "Automatic spin-entangled decays of heavy resonances in Monte Carlo simulations," JHEP **1303** (2013) 015 [arXiv:1212.3460 [hep-ph]].

[35] G. Aad *et al.* [ATLAS Collaboration], "Observation of spin correlation in $t\bar{t}$ events from pp collisions at sqrt(s) = 7 TeV using the ATLAS detector," Phys. Rev. Lett. **108** (2012) 212001 [arXiv:1203.4081 [hep-ex]]; ATLAS Collaboration, "Measurement of spin correlations in top-antitop events from proton-proton collisions at $\sqrt{s} = 7$ TeV using the ATLAS detector," ATLAS-CONF-2013-101.

[36] M. Beneke, I. Efthymiopoulos, M. L. Mangano, J. Womersley, A. Ahmadov, G. Azuelos, U. Baur and A. Belyaev *et al.*, "Top quark physics," In *Geneva 1999, Standard model physics (and more) at the LHC* 419-529 [hep-ph/0003033]; F. -P. Schilling, "Top Quark Physics at the LHC: A Review of the First Two Years," Int. J. Mod. Phys. A **27** (2012) 1230016 [arXiv:1206.4484 [hep-ex]].

[37] M. Jezabek, "Top quark physics," Nucl. Phys. Proc. Suppl. **37B** (1994) 197 [hep-ph/9406411].

[38] A. Brandenburg, Z. G. Si and P. Uwer, "QCD corrected spin analyzing power of jets in decays of polarized top quarks," Phys. Lett. B **539** (2002) 235 [hep-ph/0205023].

[39] W. Bernreuther, A. Brandenburg, Z. G. Si and P. Uwer, "Top quark spin correlations at hadron colliders: Predictions at next-to-leading order QCD," Phys. Rev. Lett. **87** (2001) 242002 [hep-ph/0107086].

[40] W. Bernreuther, A. Brandenburg, Z. G. Si and P. Uwer, "Top quark pair production and decay at hadron colliders," Nucl. Phys. B **690** (2004) 81 [hep-ph/0403035].

[41] W. Bernreuther and Z. -G. Si, "Distributions and correlations for top quark pair production and decay at the Tevatron and LHC.," Nucl. Phys. B **837** (2010) 90 [arXiv:1003.3926 [hep-ph]].

[42] T. Aaltonen *et al.* [CDF Collaboration], "Measurement of $t\bar{t}$ Spin Correlation in $p\bar{p}$ Collisions Using the CDF II Detector at the Tevatron," Phys. Rev. D **83** (2011) 031104 [arXiv:1012.3093 [hep-ex]].

[43] V. M. Abazov *et al.* [D0 Collaboration], "Evidence for spin correlation in $t\bar{t}$ production," Phys. Rev. Lett. **108** (2012) 032004 [arXiv:1110.4194 [hep-ex]].

[44] S. Chatrchyan *et al.* [CMS Collaboration], "Measurements of $t\bar{t}$ spin correlations and top-quark polarization using dilepton final states in pp collisions at $\sqrt{s} = 7$ TeV," arXiv:1311.3924 [hep-ex]; CMS Collaboration, "Measurement of Spin Correlations in ttbar production," CMS-PAS-TOP-12-004.

[45] G. Mahlon and S. J. Parke, "Angular correlations in top quark pair production and decay at hadron colliders," Phys. Rev. D **53** (1996) 4886 [hep-ph/9512264]; G. Mahlon and S. J. Parke, "Spin Correlation Effects in Top Quark Pair Production at the LHC," Phys. Rev. D **81** (2010) 074024 [arXiv:1001.3422 [hep-ph]].

[46] M. Baumgart and B. Tweedie, "A New Twist on Top Quark Spin Correlations," JHEP **1303** (2013) 117 [arXiv:1212.4888 [hep-ph]].

[47] C. Buttar, S. Dittmaier, V. Drollinger, S. Frixione, A. Nikitenko, S. Willenbrock, S. Abdullin and E. Accomando *et al.*, "Les houches physics at TeV colliders 2005, standard model and Higgs working group: Summary report," hep-ph/0604120

[48] MadGraph5_aMC@NLO, https://launchpad.net/mg5amcnlo

[49] J. Alwall, M. Herquet, F. Maltoni, O. Mattelaer and T. Stelzer, "MadGraph5 : Going Beyond," JHEP **1106** (2011) 128 [arXiv:1106.0522 [hep-ph]].

[50] T. Sjostrand, S. Mrenna and P. Z. Skands, "PYTHIA 6.4 Physics and Manual," JHEP **0605** (2006) 026 [hep-ph/0603175].